

# Ionic liquids as adjuvants for the tailored extraction of biomolecules in aqueous biphasic systems†

Jorge F. B. Pereira,<sup>a</sup> Álvaro S. Lima,<sup>b</sup> Mara G. Freire<sup>\*a</sup> and João A. P. Coutinho<sup>a</sup>

Received 24th February 2010, Accepted 13th July 2010

DOI: 10.1039/c003578e

The potential use of ionic liquids (ILs) as adjuvants in typical polymer-salt aqueous systems for the separation and purification of vital biomolecules is investigated. An innovative study involving the addition of various imidazolium-based ILs to conventional PEG/inorganic salt aqueous biphasic systems (ABS), aiming at controlling their phase behaviour and extraction capability for L-tryptophan, is carried out here. For this purpose, phase diagrams and respective tie-lines for PEG 600/Na<sub>2</sub>SO<sub>4</sub> ABS with the addition of small quantities of IL were established. In addition, the partition coefficients of L-tryptophan were determined in those systems. The results obtained indicate that the addition of small amounts of IL to the typical PEG/inorganic salt aqueous systems could largely control the extraction efficiency for L-tryptophan, and that efficiency depends on the IL employed. Salting-in inducing ILs enhance the partition coefficient of L-tryptophan for the PEG-rich phase while salting-out inducing ILs decrease the partitioning of the amino acid. These results are an interesting advance in biotechnological separation processes regarding the extraction of biomolecules that could be used instead of the common approach of PEG functionalization.

## Introduction

Polyethylene glycols (PEGs) are a class of polymers widely used in industrial processes, especially due to their high biodegradability, low toxicity, low volatility, low melting points, large water solubility and low cost. These attractive properties have prompted the use of PEGs in various processes, one of the most interesting being aqueous biphasic systems.<sup>1</sup> Aqueous biphasic systems (ABS) are a technique for the separation and purification of biological macromolecules, such as proteins,<sup>2</sup> enzymes,<sup>3</sup> antibiotics,<sup>4</sup> and alkaloids,<sup>5</sup> among others. They have been developed since the mid 1950s as mild separation methods with broad applicability in the biotechnological field,<sup>6–8</sup> and are formed by adding to water either two structurally different hydrophilic polymers, such as dextran and PEG<sup>9</sup> or maltodextrin and PEG,<sup>10</sup> or alternatively a polymer and a salting-out inducing inorganic salt, such as PEG and potassium phosphate.<sup>11</sup> Each phase of these systems becomes enriched in one of the two compounds thus creating two aqueous phases of widely different chemical and physical nature, that favour the partitioning of biomolecules between them.<sup>12</sup> The biomolecules partitioning among phases results from interactions that are surface dependent, and relies on the hydrophobicity, polarity and charge of the biomolecule that further determines to

which individual phase the biomolecule will preferentially migrate.

ABS typically formed by polymer and inorganic salt solutions have several advantages over conventional polymer-polymer ABS,<sup>13</sup> such as low interfacial tension, good biocompatibility, fast and high phase separation rates and low cost, which makes them more viable for downstream processing. However, the hydrophilic nature of PEG limits the applicability of this technique when the goal is to extract hydrophobic biomolecules. To overcome this limitation one possible approach used by some researchers has been the functionalization of PEG.<sup>14–19</sup> Rosa *et al.*<sup>16</sup> and Azevedo *et al.*<sup>17</sup> applied the functionalization of PEG process to the purification of human immunoglobulin, while Jiang *et al.*<sup>18</sup> have used an ionic liquid functionalized PEG for the extraction of penicillin. The last approach<sup>18</sup> allowed the modification of the polymer-rich phase hydrophilicity enhancing the recovery of penicillin. Moreover, Wu *et al.*<sup>19</sup> have also recently shown that PEG can be functionalized with ionic liquids, for enhanced extraction and polymer recovery. In summary, those works<sup>16–19</sup> were aimed at tuning the properties of PEG through the modification of its chemical structure.

A novel approach to ABS, originally proposed by Rogers and co-workers,<sup>20</sup> was the use of ionic liquids (ILs) as possible alternatives to polymer-based systems. ILs are a new class of purely ionic salt-like materials with melting points below 100 °C.<sup>21</sup> The main characteristics of ILs include high solvation abilities<sup>22</sup> and coordination properties, general non flammability, high thermal<sup>23</sup> and chemical stabilities and negligible vapour pressures.<sup>24</sup> All of these encouraging properties have led, over the last decade, to research on ILs as alternative solvents for the replacement of the noxious volatile organic compounds routinely used in industry. Of particular interest is the high

<sup>a</sup>CICECO, Departamento de Química, Universidade de Aveiro, Campus Universitário de Santiago, 3810-193, Aveiro, Portugal. E-mail: maragfreire@ua.pt; Fax: +351-234-370084; Tel: +351-234-401507

<sup>b</sup>Programa de Pós-Graduação em Engenharia de Processos, Universidade Tiradentes. Av. Murilo Dantas, 300. CEP: 49032-490, Aracaju-Sergipe, Brasil

† Electronic supplementary information (ESI) available: Experimental binodal curve mass fraction data. See DOI: 10.1039/c003578e

degree of tunability of the physical and chemical properties by varying the chemical structures of the ions comprised in the IL. Recently we have shown that a wide number of ILs, in the presence of inorganic salts, could be used to prepare ABS, and we have studied their impact on ABS formation and extraction aptitude for biomolecules.<sup>25–27</sup> It was observed that, as for other applications, it is possible to control the ABS physicochemical properties by a wise combination of IL cations and/or anions, thus making possible the manipulation of the properties of the extraction phases for enhanced yield of product recovery.<sup>25–27</sup> Indeed, a number of works on the extraction of biomolecules with IL-based ABS have been reported within the last couple of years.<sup>25–32</sup>

Aimed at developing an alternative technique for modification of the PEG-rich phase characteristics, a new approach making use of ILs is proposed. Instead of the PEG functionalization, the IL is used here as a promoter or adjuvant of ABS formation aimed at tuning the intrinsic properties of the aqueous phases. The formation of PEG-sodium sulfate ABS, and their phase behaviour, in the presence of various ILs, is investigated. Moreover, the effect of adding distinct ILs as adjuvants for the extraction ability of archetypal ABS is evaluated here using L-tryptophan as a model biomolecule. Influences of IL and inorganic salt concentration, temperature, and pH of the medium were discussed throughout the partition coefficients obtained.

## Results and discussion

### Phase diagrams and tie-lines

The chemical structures of the studied imidazolium-based ILs are depicted in Fig. 1. We have focused on the subgroup of imidazolium halides to evaluate the impact of IL cation on the separations, and on the 1-butyl-3-methylimidazolium cation,  $[C_4mim]^+$ , combined with a variety of anions, to analyze their

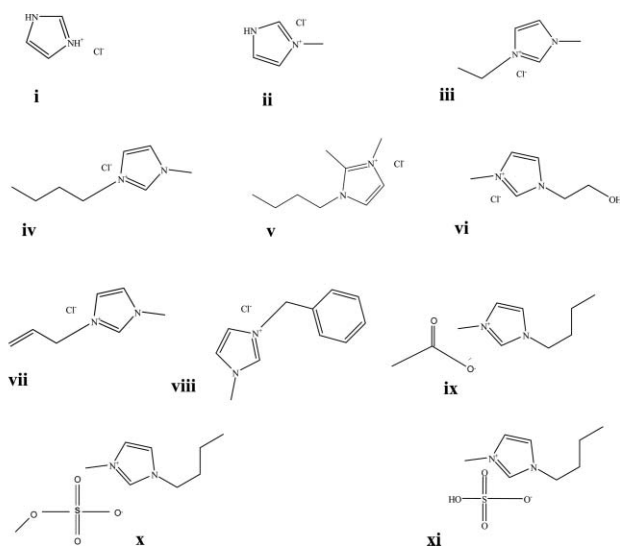


**Fig. 1** Chemical structures of the studied ILs: (i) [im]Cl; (ii) [C<sub>1</sub>im]Cl; (iii) [C<sub>2</sub>mim]Cl; (iv) [C<sub>4</sub>mim]Cl; (v) [C<sub>4</sub>C<sub>1</sub>mim]Cl; (vi) [OHC<sub>2</sub>mim]Cl; (vii) [amim]Cl; (viii) [C<sub>7</sub>H<sub>7</sub>mim]Cl; (ix) [C<sub>4</sub>mim][CH<sub>3</sub>CO<sub>2</sub>]; (x) [C<sub>4</sub>mim][MeSO<sub>4</sub>]; (xi) [C<sub>4</sub>mim][HSO<sub>4</sub>].

influence on the liquid–liquid phase diagrams and L-tryptophan extraction ability.

Fig. 2 to 4 present the experimental phase diagrams at 298 K and atmospheric pressure, for each PEG 600 + Na<sub>2</sub>SO<sub>4</sub> + H<sub>2</sub>O + 5 wt% IL system (*cf.* Supporting Information with experimental weight fraction data†). It should be pointed out that the IL concentration was kept constant in all phase diagrams. The binodal curves are reported in molality units for an enhanced understanding on the impact of distinct ILs in the formation of ABS. Fig. 2 shows the influence of the IL cation alkyl chain length, as well as the number of alkyl substitutions at the cation, in the binodal curves using different ILs, namely [im]Cl, [C<sub>1</sub>im]Cl, [C<sub>2</sub>mim]Cl, [C<sub>4</sub>mim]Cl and [C<sub>4</sub>C<sub>1</sub>mim]Cl. Fig. 3 describes the effect of the presence of diverse functional groups at the IL cation through the binodal curves, with results for [OHC<sub>2</sub>mim]Cl, [amim]Cl and [C<sub>7</sub>H<sub>7</sub>mim]Cl. Finally, Fig. 4 evaluates the influence of the IL anion nature in the phase diagrams, where results for [C<sub>4</sub>mim]Cl, [C<sub>4</sub>mim][CH<sub>3</sub>CO<sub>2</sub>], [C<sub>4</sub>mim][MeSO<sub>4</sub>] and [C<sub>4</sub>mim][HSO<sub>4</sub>] are depicted. In all figures the binodal curve for the control system without IL is further represented for comparison.

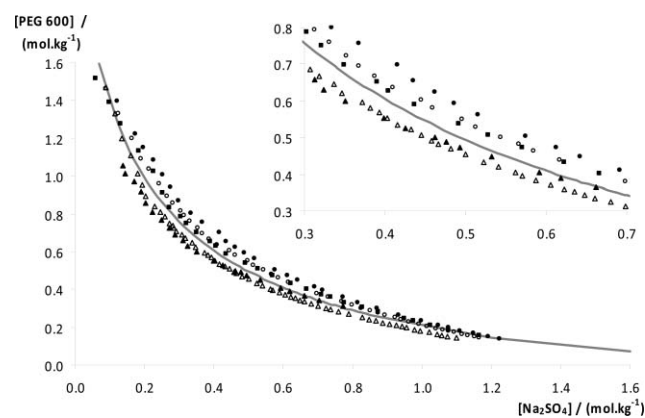


**Fig. 2** Phase diagrams for the imidazolium-based quaternary systems composed of PEG 600 + Na<sub>2</sub>SO<sub>4</sub> + H<sub>2</sub>O + 5 wt% IL at 298 K: (—) no IL; (●) [im]Cl; (○) [C<sub>1</sub>im]Cl; (■) [C<sub>2</sub>mim]Cl; (△) [C<sub>4</sub>mim]Cl; (▲) [C<sub>4</sub>C<sub>1</sub>mim]Cl.

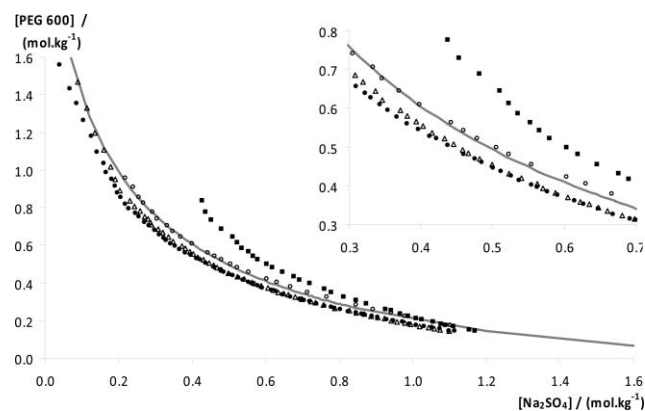


**Fig. 3** Phase diagrams for the imidazolium-based quaternary systems composed of PEG 600 + Na<sub>2</sub>SO<sub>4</sub> + H<sub>2</sub>O + 5 wt% IL at 298 K: (—) no IL; (△) [C<sub>4</sub>mim]Cl; (■) [OHC<sub>2</sub>mim]Cl; (○) [amim]Cl; (●) [C<sub>7</sub>H<sub>7</sub>mim]Cl.

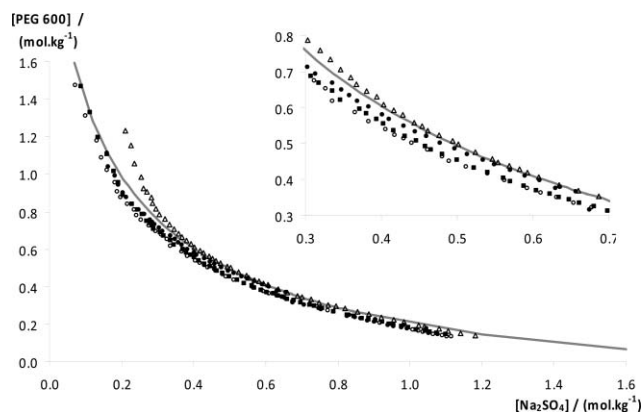


**Fig. 4** Phase diagrams for the imidazolium-based quaternary systems composed of PEG 600 + Na<sub>2</sub>SO<sub>4</sub> + H<sub>2</sub>O + 5 wt% IL at 298 K: (—) no IL; (■) [C<sub>4</sub>mim]Cl; (●) [C<sub>4</sub>mim][CH<sub>3</sub>CO<sub>2</sub>]; (○) [C<sub>4</sub>mim][MeSO<sub>4</sub>]; (△) [C<sub>4</sub>mim][HSO<sub>4</sub>].

It is known that an increase of the ILs' hydrophobic nature leads to a lower affinity for water,<sup>33–35</sup> and consequently, to an enhanced phase separation in IL-based ABS.<sup>25–26</sup> Fig. 2 shows how an increase in the cation alkyl chain length from [C<sub>2</sub>mim]Cl to [C<sub>4</sub>mim]Cl, and the presence of more alkyl substitutions on the cation, reduces the phases' miscibility. In contrast, in Fig. 3 it is shown that the introduction of a terminal hydroxyl group or a double bond at the alkyl chain confers a polar character to the IL, reducing the degree of phase separation. The effect of the IL on the binodal curves reported in Fig. 2 and 3 thus follows a trend imposed by the IL hydrophobicity. The increase in the cation chain length and number of alkyl substitutions leads to a larger immiscibility, although only ILs larger than [C<sub>4</sub>mim]Cl present two-phase regions larger than that observed for the ABS with no IL.

The results for the [C<sub>4</sub>mim]-based ILs, sketched in Fig. 4, show the impact of the IL anion on the ABS formation. Only the IL [C<sub>4</sub>mim][HSO<sub>4</sub>] increases the phases' miscibility when compared to the pure system with no IL. All the other ILs induced a larger phase separation. The trend for the anion increasing immiscibility between the two phases is identical to that previously reported by Ventura *et al.*<sup>26</sup> for IL-based ABS formation. There is a decrease on the ABS formation ability with the increase in the IL anion affinity for water, following the trend of the anion hydrogen bond acidity.<sup>26</sup> As observed for the IL cations, the hydrophobicity of the IL anion also controls the ABS formation ability.

The experimental binodal curves were correlated using the empirical relationship described by eqn (1)<sup>35</sup>

$$Y = A \exp(BX^{0.5}) - (CX^3) \quad (1)$$

where  $Y$  and  $X$  are respectively, the PEG and inorganic salt weight percentages, and  $A$ ,  $B$  and  $C$  are constants obtained by the regression of the experimental data. The fitted parameters, and respective standard deviations, are summarized in Table 1. The experimental tie-lines (TLs) measured for each system along with the respective tie-line lengths (TLLs) are reported in Table 2. An example of the TLs measured in this work is provided in Fig. 5 along with the binodal curve for the system PEG 600 + Na<sub>2</sub>SO<sub>4</sub> + H<sub>2</sub>O + 5 wt% [C<sub>2</sub>mim]Cl.

**Table 1** Correlation parameters used in eqn (1) to describe the binodals (and respective standard deviations,  $\sigma$ ) for the PEG 600 + Na<sub>2</sub>SO<sub>4</sub> + H<sub>2</sub>O + 5 wt% IL quaternary systems at 298 K

Quaternary System	( $A \pm \sigma$ )	( $B \pm \sigma$ )	$10^5(C \pm \sigma)$
No IL	81.8 ± 0.6	-0.471 ± 0.004	20.0 ± 0.6
[im]Cl	79.1 ± 1.2	-0.405 ± 0.008	20.0 ± 0.9
[C <sub>1</sub> mim]Cl	75.7 ± 0.8	-0.405 ± 0.006	30.0 ± 0.7
[C <sub>2</sub> mim]Cl	70.8 ± 1.7	-0.381 ± 0.014	30.0 ± 2.3
[C <sub>4</sub> mim]Cl	83.3 ± 0.5	-0.506 ± 0.003	20.0 ± 0.5
[C <sub>4</sub> C <sub>1</sub> mim]Cl	73.2 ± 1.1	-0.457 ± 0.009	10.0 ± 2.2
[OHC <sub>2</sub> mim]Cl	155.8 ± 6.4	-0.645 ± 0.018	20.0 ± 1.3
[amim]Cl	84.4 ± 1.1	-0.485 ± 0.006	10.0 ± 0.7
[C <sub>7</sub> H <sub>7</sub> mim]Cl	72.4 ± 0.8	-0.448 ± 0.006	20.0 ± 1.1
[C <sub>4</sub> mim][CH <sub>3</sub> CO <sub>2</sub> ]	76.4 ± 1.4	-0.452 ± 0.100	20.0 ± 1.7
[C <sub>4</sub> mim][MeSO <sub>4</sub> ]	77.1 ± 0.5	-0.476 ± 0.004	20.0 ± 0.5
[C <sub>4</sub> mim][HSO <sub>4</sub> ]	105.5 ± 1.6	-0.576 ± 0.007	10.0 ± 0.7

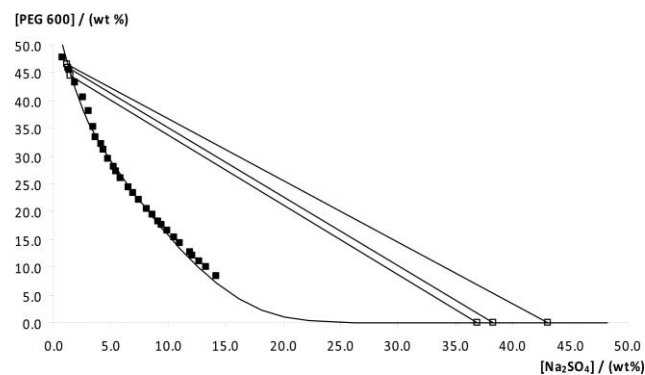


**Fig. 5** Phase diagram for the PEG 600 + Na<sub>2</sub>SO<sub>4</sub> + H<sub>2</sub>O + 5 wt% [C<sub>2</sub>mim]Cl quaternary system at 298 K: (■) binodal curve data; (—) binodal adjusted curve; (□) TL data.

### Partitioning of the ILs in the ABS

As could be expected, the ILs added to the ABS also partition themselves between the two phases according to their physical and chemical nature. For a better understanding of their impact on the phase separation and on the extraction ability of the ABS, the ILs' distribution between the two aqueous phases was also evaluated. The partition coefficient of each IL,  $K_{IL}$ , is defined as the ratio of the IL concentration in the PEG 600 and that in the Na<sub>2</sub>SO<sub>4</sub>-rich phase, as described by eqn (2):

$$K_{IL} = \frac{[IL]_{PEG600}}{[IL]_{Na_2SO_4}} \quad (2)$$

where  $[IL]_{PEG600}$  and  $[IL]_{Na_2SO_4}$  are the concentrations of IL in the polymer and in the inorganic salt aqueous phases, respectively.

The partition coefficients of each IL at 298.15 K are reported in Table 3. In addition, the mass fraction compositions of each component at which the partition coefficients were determined are also presented in Table 3. With the exception of [im]Cl, all ILs present partition coefficients larger than 1, indicating that ILs will partition preferentially for the PEG-rich phase. Certainly, [im]Cl is the strongest salting-out inducing IL evaluated, and thus preferentially partitions for the inorganic-salt-rich phase, while the intensity of the partitioning of the IL is proportional to the IL salting-in/-out ability. Salting-out inducing ions (high charge density ions) have a greater tendency to form

**Table 2** Initial mass fraction compositions for the TLs and TLLs determination, and compositions of the respective top (*T*) and bottom (*B*) phases at 298 K

Quaternary System	Mass Fraction Composition/(wt%)		$Y_T$	$X_T$	$Y_B$	$X_B$	TLL
	PEG 600	Na <sub>2</sub> SO <sub>4</sub>					
no IL	40.00	5.04	45.98	1.49	0.06	28.72	53.38
	39.94	7.04	50.56	1.04	0.04	29.58	58.02
[im]Cl	40.04	5.02	44.53	2.00	0.01	31.85	53.60
	40.30	6.97	48.39	1.47	0.00	34.38	58.51
[C <sub>1</sub> im]Cl	39.96	7.04	48.64	1.19	0.00	34.00	58.67
[C <sub>2</sub> mim]Cl	39.97	5.10	44.52	1.48	0.00	36.90	56.89
	39.95	6.04	45.83	1.30	0.00	38.27	58.88
[C <sub>4</sub> mim][Cl]	40.09	7.01	46.54	1.21	0.00	43.03	62.56
	40.15	5.01	45.14	1.46	0.00	33.50	55.36
[C <sub>4</sub> C <sub>1</sub> mim]Cl	40.18	6.00	46.64	1.31	0.00	35.10	57.60
	39.93	5.02	44.70	1.17	0.02	37.24	57.42
[OHC <sub>2</sub> mim]Cl	39.97	6.04	45.31	1.10	0.00	42.96	61.68
	40.04	5.07	44.67	3.70	6.56	14.98	39.75
[amim]Cl	40.07	6.99	49.93	3.08	0.74	22.55	52.90
	40.13	5.99	44.00	1.80	0.00	49.49	64.88
[C <sub>7</sub> H <sub>7</sub> mim]Cl	40.13	7.00	45.09	1.67	0.00	50.10	66.17
	39.94	5.03	45.52	1.07	0.00	33.40	55.83
[C <sub>4</sub> mim][CH <sub>3</sub> CO <sub>2</sub> ]	40.03	7.00	49.19	0.74	0.00	34.32	59.56
	39.93	6.10	47.14	1.14	0.00	33.60	57.23
[C <sub>4</sub> mim][MeSO <sub>4</sub> ]	39.95	7.03	47.84	1.07	0.00	37.20	59.95
	39.98	5.01	44.47	1.34	0.00	37.71	57.45
[C <sub>4</sub> mim][HSO <sub>4</sub> ]	39.99	5.06	44.78	2.21	0.45	28.72	51.64
	40.10	7.13	48.10	1.86	0.09	33.52	57.51

**Table 3** Partition coefficients of each IL ( $K_{IL}$ ) and mass fraction compositions of the quaternary systems at 298.15 K

Quaternary System	Mass Fraction Composition/(wt%)			$K_{IL}$
	PEG 600	Na <sub>2</sub> SO <sub>4</sub>	IL	
[im]Cl	39.96	5.00	5.08	0.48
[C <sub>1</sub> mim]Cl	40.12	5.00	5.00	2.23
[C <sub>2</sub> mim]Cl	39.98	5.01	5.03	4.80
[C <sub>4</sub> mim]Cl	40.02	5.00	5.01	7.04
[C <sub>7</sub> H <sub>7</sub> mim]Cl	39.94	5.06	5.00	15.02
[C <sub>4</sub> C <sub>1</sub> mim]Cl	42.98	4.76	4.81	13.80
[amim]Cl	39.98	5.04	4.99	2.91
[OHC <sub>2</sub> mim]Cl	39.97	5.02	5.01	2.21
[C <sub>4</sub> mim][HSO <sub>4</sub> ]	39.99	5.04	5.06	6.64
[C <sub>4</sub> mim][CH <sub>3</sub> CO <sub>2</sub> ]	39.98	5.08	5.06	7.34
[C <sub>4</sub> mim][MeSO <sub>4</sub> ]	39.98	5.01	5.00	8.74

hydration complexes when compared to salting-in inducing ions (low charge density ions). Therefore, the ions' aptitude to form hydration complexes, and thus affinity for aqueous environments, will define the phase for which the IL ions mainly migrate.<sup>36</sup> This IL migration for a particular phase will naturally change the chemical and physical properties of such a phase, and as will be shown below, such IL partitioning is responsible for the enhanced extraction ability of L-tryptophan observed in several ABS. Although outside the scope of this work it is interesting to note that these results suggest the possibility of using PEG-based ABS to remove hydrophilic ILs from aqueous solutions, providing an interesting approach to the treatment of aqueous effluents contaminated with ILs.

A comparison between the ILs' partition coefficients reported in Table 3 and the binodal curves sketched in Fig. 2 to 4 indicate that the addition of 5 wt% of IL to ABS enlarges the biphasic region of the PEG 600 + Na<sub>2</sub>SO<sub>4</sub> + H<sub>2</sub>O system when the IL

displays a  $K_{IL} > 7.0$ , while the opposite result is obtained when  $K_{IL} < 7.0$ .

### Partitioning of L-tryptophan in the ABS

Tryptophan (C<sub>11</sub>H<sub>12</sub>N<sub>2</sub>O<sub>2</sub>) is an essential amino acid that has to be added into animal feed, since its synthesis cannot be achieved by animals. The body uses tryptophan to produce niacin and serotonin.<sup>37</sup> Its chemical structure is formed by an indole group that confers the hydrophobic characteristics to the amino acid. Even so, L-tryptophan was used in this work as a model biomolecule and as a proof of principle to the proposed technique. In this context, these novel systems can be further explored through their selective extraction capability with a wide range of biomolecules of interest.

The partition coefficient of L-tryptophan,  $K_{Trp}$ , is defined here as the ratio of the concentration of L-tryptophan in the polymer and salt-rich phases and as described by eqn (3):

$$K_{Trp} = \frac{[Trp]_{PEG600}}{[Trp]_{Na_2SO_4}} \quad (3)$$

where  $[Trp]_{PEG600}$  and  $[Trp]_{Na_2SO_4}$  are the concentration of L-tryptophan in the PEG 600 and Na<sub>2</sub>SO<sub>4</sub> aqueous-rich phases, respectively.

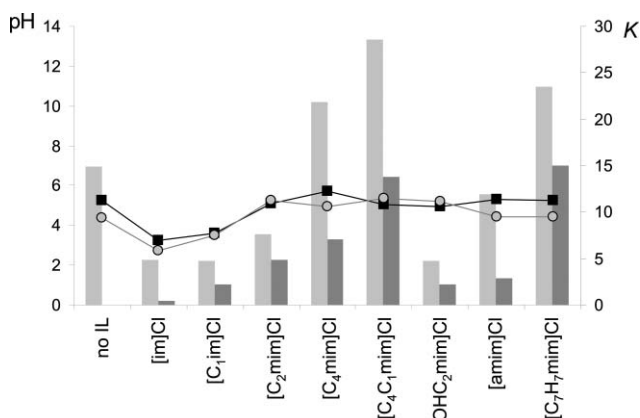
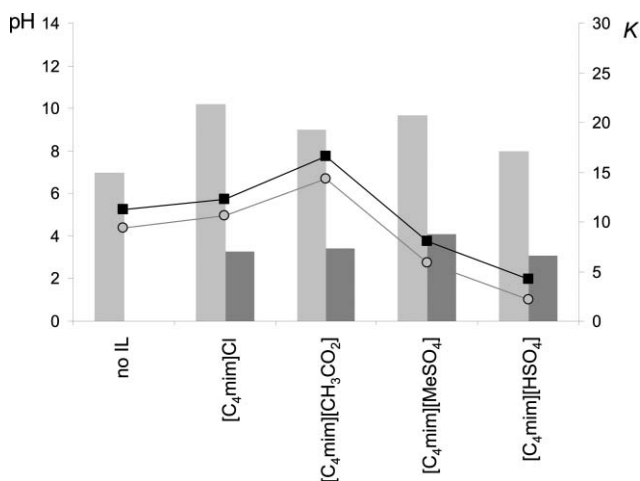
The partition coefficients of biomolecules in ABS are dependent on hydrophobic type interactions, electrostatic forces, molecular size, solubility, and affinity for both phases, and their magnitudes further depend on the two-phase compositions and on the nature of the biomolecules.<sup>6,38–39</sup> The partition coefficients of L-tryptophan ( $K_{Trp}$ ) at 298.15 K in the studied ABS, and respective systems' composition, are reported in Table 4. The reproducibility of the measurements was evaluated with the

**Table 4** Partition coefficients of L-tryptophan ( $K_{\text{Trp}}$ ) and mass fraction compositions of the quaternary systems at 298.15 K

Quaternary System	Mass Fraction Composition/(wt%)			$K_{\text{Trp}}$
	PEG 600	Na <sub>2</sub> SO <sub>4</sub>	IL	
no IL	40.00	5.04	—	14.93
	39.96	6.04	—	16.72
	39.94	7.04	—	20.54
[im]Cl	40.04	5.02	5.04	4.82
	39.84	6.06	5.26	5.28
	40.30	6.97	5.04	7.27
[C <sub>1</sub> im]Cl	40.01	5.01	5.04	4.69
	40.08	6.01	5.00	5.55
	39.96	7.04	5.07	6.01
[C <sub>2</sub> mim]Cl	39.97	5.10	5.01	7.63
	39.95	6.04	5.29	8.69
	40.09	7.01	5.04	9.11
[C <sub>4</sub> mim]Cl	40.15	5.01	4.98	21.84
	40.18	6.00	5.05	29.43
	40.01	7.00	5.00	37.03
[C <sub>4</sub> C <sub>1</sub> mim]Cl	39.93	5.02	5.14	28.62
	39.97	6.04	5.00	31.21
	40.21	6.97	5.05	32.11
[OHC <sub>2</sub> mim]Cl	40.04	5.07	5.00	4.72
	40.15	6.04	5.06	5.51
	40.07	6.99	5.20	5.71
[amim]Cl	39.93	5.01	5.08	11.88
	40.13	5.99	5.00	14.85
	40.13	7.00	5.07	13.06
[C <sub>7</sub> H <sub>7</sub> mim]Cl	39.94	5.03	5.00	23.46
	40.04	6.00	5.03	29.57
	40.03	7.00	5.11	42.47
[C <sub>4</sub> mim][CH <sub>3</sub> CO <sub>2</sub> ]	39.97	5.01	4.96	19.24
	39.93	6.10	5.04	29.83
	39.95	7.03	4.96	34.81
[C <sub>4</sub> mim][MeSO <sub>4</sub> ]	39.98	5.01	5.03	20.76
	40.08	5.99	5.00	25.76
	40.04	7.01	5.00	32.64
[C <sub>4</sub> mim][HSO <sub>4</sub> ]	39.99	5.06	5.02	17.08
	40.16	5.99	5.15	21.28
	40.10	7.13	5.03	36.28

PEG 600 + Na<sub>2</sub>SO<sub>4</sub> + water system without IL addition, and the average uncertainty associated to the L-tryptophan partition coefficients is within  $\pm 5\%$ . The  $K_{\text{Trp}}$  dependence on the IL cation and anion, at 298.15 K, is displayed in Fig. 6 and Fig. 7. For all cases,  $K_{\text{Trp}}$  is larger than 1.0, denoting the amino acid's preferential partitioning for the PEG-rich phase (hydrophobic phase). Typical solute-solvent interactions are likely to involve van der Waals forces, electrostatic interactions, hydrogen-bonding and  $\pi \cdots \pi$  stacking. The presence of the IL enhances this type of interactions allowing the manipulation of the characteristics and the extraction ability by the polymer-rich phase. Moreover, the protons of the imidazolium ring can act as proton donors while the counterions are typically proton accepting anions.

The  $K_{\text{Trp}}$  observed for the systems using ILs with salting-out inducing characteristics were smaller than those obtained for the ABS reference system without IL, but it showed a strong increase with the alkyl-chain size of the cation (*e.g.* from 4.82 with [im]Cl to 21.84 with [C<sub>4</sub>mim]Cl in the system using 40 wt% PEG 600 + 5 wt% Na<sub>2</sub>SO<sub>4</sub> + 5 wt% IL). This trend follows the IL salting-in/-out inducing ability. While salting-out ILs such as [im]Cl, [C<sub>1</sub>im]Cl, [C<sub>2</sub>mim]Cl, [OHC<sub>2</sub>mim]Cl and [amim]Cl reduce  $K_{\text{Trp}}$ , the remaining ILs increase the partitioning of the amino acid

**Fig. 6** Partition coefficients of L-tryptophan ( $K_{\text{Trp}}$ ) (light grey) and of each IL ( $K_{\text{IL}}$ ) (dark grey), and pH of both top (black squares) and bottom phases (grey circles) for the chloride-based systems composed of 40 wt% PEG 600 + 5 wt% Na<sub>2</sub>SO<sub>4</sub> + H<sub>2</sub>O + 5 wt% IL, at 298.15 K.**Fig. 7** Partition coefficients of L-tryptophan ( $K_{\text{Trp}}$ ) (light grey) and of each IL ( $K_{\text{IL}}$ ) (dark grey), and pH of both top (black squares) and bottom (grey circles) phases, for the [C<sub>4</sub>mim]-based systems composed of 40 wt% PEG 600 + 5 wt% Na<sub>2</sub>SO<sub>4</sub> + H<sub>2</sub>O + 5 wt% IL, at 298.15 K.

(salting-in inducing ILs). In addition, removing the most acidic hydrogen at the C<sub>2</sub> position of the IL by increasing the number of alkyl chain substitutions, as in [C<sub>4</sub>C<sub>1</sub>mim]Cl, leads to a higher  $K_{\text{Trp}}$  when compared to [C<sub>4</sub>mim]Cl.

It seems that it is mainly the IL partition to the PEG-rich phase that improves the partitioning of L-tryptophan. Indeed, it can be seen in Fig. 6 that there is a close agreement between  $K_{\text{Trp}}$  and  $K_{\text{IL}}$ , meaning that it is the presence of the IL on the PEG-rich phase that enhances the partitioning of the amino acid. Moreover, the presence of benzyl groups or double bonds at the IL cation also enhances the ability of the PEG-rich phase for extracting the amino acid. Remarkable are the results obtained for [C<sub>7</sub>H<sub>7</sub>mim]Cl where  $K_{\text{Trp}}$  takes the value 23.46 for the system composed of 40 wt% PEG 600 + 5 wt% Na<sub>2</sub>SO<sub>4</sub> + 5 wt% IL, or 42.47 for the system containing 40 wt% PEG 600 + 7 wt% Na<sub>2</sub>SO<sub>4</sub> + 5 wt% IL. In this particular case, it appears that the additional contributions of  $\pi \cdots \pi$  interactions of a second aromatic ring are responsible for the increase in the  $K_{\text{Trp}}$  values.

The observed influence of the IL anion follows the anion hydrophobicity<sup>26</sup> but it is minor when compared with the

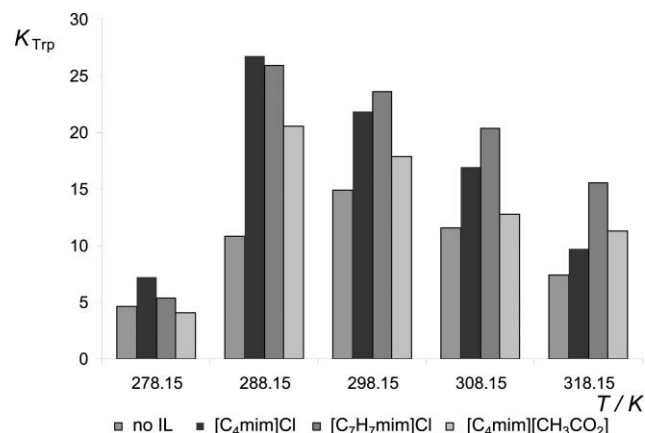
**Table 5** Partition coefficients of L-tryptophan ( $K_{\text{Trp}}$ ) and mass fraction compositions of the quaternary systems at different temperatures

Quaternary System	$T/K$	Mass Fraction Composition/(wt%)			$K_{\text{Trp}}$
		PEG 600	$\text{Na}_2\text{SO}_4$	IL	
no IL	278.15	40.07	5.18	—	4.62
	288.15	39.89	5.16	—	10.87
	298.15	40.00	5.04	—	14.93
	308.15	39.97	5.06	—	11.60
	318.15	39.92	5.08	—	7.45
[C <sub>4</sub> mim]Cl	278.15	40.04	5.08	5.12	7.24
	288.15	39.91	5.06	5.05	26.77
	298.15	40.15	5.01	4.98	21.84
	308.15	40.16	5.03	4.99	16.96
	318.15	40.24	5.01	5.03	9.74
[C <sub>7</sub> H <sub>7</sub> mim]Cl	278.15	39.88	5.00	5.07	5.33
	288.15	39.95	5.01	5.12	25.90
	298.15	39.94	5.03	5.00	23.46
	308.15	39.95	5.12	5.08	20.41
	318.15	40.25	5.04	5.06	15.52
[C <sub>4</sub> mim][CH <sub>3</sub> CO <sub>2</sub> ]	278.15	39.92	5.02	4.98	4.11
	288.15	39.73	4.99	5.28	20.52
	298.15	39.97	5.01	4.96	19.24
	308.15	40.01	5.05	5.31	12.76
	318.15	40.03	5.05	5.00	11.28

influence of the IL cation. The  $K_{\text{Trp}}$  observed for the various [C<sub>4</sub>mim]-based ILs studied are similar to those observed for [C<sub>4</sub>mim]Cl. Therefore, the IL cation plays a major role in controlling the PEG-rich phase extraction ability for L-tryptophan. This effect is identical to what was observed for IL-based ABS previously studied by us.<sup>25–26</sup>

Previously, Pei *et al.*<sup>40</sup> reported that the temperature significantly influences the extraction efficiency of proteins. Therefore, aimed at evaluating the temperature influence in the extraction of L-tryptophan, four systems were selected (those containing no IL, [C<sub>4</sub>mim]Cl, [C<sub>7</sub>H<sub>7</sub>mim]Cl and [C<sub>4</sub>mim][CH<sub>3</sub>CO<sub>2</sub>]).  $K_{\text{Trp}}$  was determined at the following temperatures: 278.15, 288.15, 298.15, 308.15 and 318.15 K. These systems allowed us to study the temperature effect upon the separation, in combination with different cations and anions. The data gathered, and accurate mass fraction compositions for each system, are displayed in Table 5. The associated uncertainty to the experimental measurements was determined with the 40 wt% PEG 600 + 5 wt% Na<sub>2</sub>SO<sub>4</sub> + 5 wt% [C<sub>4</sub>mim]Cl system (3 independent equilibration samples for each temperature assessed) and shown to be inferior to 5%. The  $K_{\text{Trp}}$  dependence on temperature is displayed in Fig. 8. The four systems, and at all temperatures, present a  $K_{\text{Trp}}$  larger than 1.0. The results indicate that the temperature has a significant effect in the amino acid partitioning. Indeed, for the system without IL there is a maximum in  $K_{\text{Trp}}$  at temperatures close to 298.15 K, while for the systems containing IL, this maximum is observed at 288.15 K. Both IL cation and anion contribute to the differences observed in the partition coefficients and their dependence on temperature. Since electrostatic contributions are rather independent on temperature, the main deviations in  $K_{\text{Trp}}$  as a function of temperature should be a consequence of dispersive forces and H-bonding interactions taking place in those systems.

From a thermodynamics perspective, the partitioning of L-tryptophan can be regarded as a process of mass transfer from

**Fig. 8** Partition coefficients of L-tryptophan ( $K_{\text{Trp}}$ ) at different temperatures.

the inorganic-salt-rich phase to the PEG-rich phase. The amino acid thermodynamic parameters of transfer, namely the standard molar Gibbs energy ( $\Delta_{\text{tr}}G_m^0$ ), the standard molar enthalpy ( $\Delta_{\text{tr}}H_m^0$ ), and the standard molar entropy of transfer ( $\Delta_{\text{tr}}S_m^0$ ), were determined through the application of the following eqns:<sup>41</sup>

$$\ln(K_{\text{Trp}}) = -\frac{\Delta_{\text{tr}}H_m^0}{R} \times \frac{1}{T} + \frac{\Delta_{\text{tr}}S_m^0}{R} \quad (4)$$

$$\Delta_{\text{tr}}G_m^0 = \Delta_{\text{tr}}H_m^0 - T\Delta_{\text{tr}}S_m^0 \quad (5)$$

$$\Delta_{\text{tr}}G_m^0 = -RT\ln(K_{\text{Trp}}) \quad (6)$$

where  $K_{\text{Trp}}$  is the partition coefficient of L-tryptophan between the Na<sub>2</sub>SO<sub>4</sub>-rich and the PEG-rich phases,  $R$  is the universal gas constant, and  $T$  is the temperature. The enthalpic and entropic contributions can be directly deduced from the linear approximation of  $\ln(K_{\text{Trp}})$  versus  $T^{-1}$ . It should be remarked that this linear function was only applied to the partition coefficient results equal to, and above, the maximum.

The plots of  $\ln(K_{\text{Trp}})$  versus  $T^{-1}$  exhibit linearity indicating that the molar enthalpy of transfer of L-tryptophan is temperature independent. The molar thermodynamic functions of transfer at 298.15 K, obtained by the linear least-square analysis, are summarized in Table 6. For all the systems studied,  $\Delta_{\text{tr}}G_m^0$  is shown to be negative, which in turn reflects the spontaneous and preferential partitioning of the amino acid for the PEG-rich phase. In addition, there is an increase in the absolute values of  $\Delta_{\text{tr}}G_m^0$  in the presence of IL when compared to the system with no IL. On the other hand, the  $\Delta_{\text{tr}}H_m^0$  negative values reveal that the transfer of L-tryptophan between the Na<sub>2</sub>SO<sub>4</sub>-rich phase and the

**Table 6** Standard molar thermodynamic functions of transfer of L-tryptophan at 298.15 K

Quaternary System	$\Delta_{\text{tr}}H_m^0$ kJ mol <sup>-1</sup>	$\Delta_{\text{tr}}S_m^0$ J mol <sup>-1</sup> K <sup>-1</sup>	$T \times \Delta_{\text{tr}}S_m^0$ J mol <sup>-1</sup>	$\Delta_{\text{tr}}G_m^0$ kJ mol <sup>-1</sup>	$\ln(K_{\text{Trp}})$
no IL	-27.34	-68.94	-20.55	-6.79	2.74
[C <sub>4</sub> mim]Cl	-24.86	-58.26	-17.37	-7.49	3.02
[C <sub>7</sub> H <sub>7</sub> mim]Cl	-12.73	-16.76	-5.00	-7.74	3.12
[C <sub>4</sub> mim][CH <sub>3</sub> CO <sub>2</sub> ]	-16.25	-31.09	-9.27	-6.99	2.82

PEG-rich phase is an exothermic process, either for the system without IL and those containing 5 wt% of IL. The standard molar enthalpies of transfer largely depend on the IL cation, such as  $[C_7H_7mim]^+$ , while the effect of changing the IL anion is mainly relevant for systems containing more complex anions, such as  $[CH_3CO_2]^-$ . Nevertheless, it is clear that the presence of  $[C_7H_7mim]Cl$  increases the overall molar enthalpy of transfer in the system, increasing therefore the partition coefficient of the amino acid. These results suggest - and as verified before with the experimental partition coefficient values - that the partitioning process is essentially controlled by the IL cation interactions with the solute. However, the presence of anions with a stronger proton accepting ability, such as  $[CH_3CO_2]^-$  (compared to  $Cl^-$ ), leads to an increase in the molar enthalpy of transfer. Yet, this increase does not directly reflect an increase in  $K_{Trp}$  since, on the other hand, there is an increase of  $\Delta_{tr}S_m^0$  when using these more complex anions. The inclusion of the IL strongly affects the molar entropy of the initial ternary system. In fact there is an increase in the L-tryptophan molar entropy of transfer following the rank:  $[C_4mim]Cl < [C_4mim][CH_3CO_2] < [C_7H_7mim]Cl$ .

In summary, the absolute results of  $T \times \Delta_{tr}S_m^0$  are inferior to  $\Delta_{tr}H_m^0$  suggesting that the enthalpic changes are the main driving forces ruling the amino acid partitioning.

The results obtained in this work suggest that the characteristics of the polymer-rich phase can be manipulated by the introduction of a small amount of an adequate IL into the system. The characteristics of the IL cation can be used to either intensify or reduce the hydrophobic character of the PEG-rich phase, or to add to it a particular type of interaction that will allow the extraction of the most diverse molecules of interest.

As shown in previous work,<sup>42</sup> the extraction of L-tryptophan is strongly affected by the pH of the medium. To rule out pH effects on the measured partition coefficients, the pH of both top and bottom phases for all the ABS studied at 298 K were measured. The pH values are presented in Fig. 6 and Fig. 7 together with the partition coefficient results. The pH values observed clearly reflect the acidic or alkaline character of the IL. For instance, lower pH values are observed for  $[C_4mim][HSO_4]$  compared to  $[C_4mim]Cl$ . In addition, no significant variations in the pH values are observed for the chloride-based series, meaning that structural and functional differences at the imidazolium cation do not alter significantly their acidic/alkaline characteristics. Although the pH value of the phases is somewhat influenced by the ILs, the pH variations are too small to affect the L-tryptophan partition. Previously<sup>42</sup> we have shown that acidic conditions (in a pH range from 1 to 3) enhance the partition coefficient of L-tryptophan, and here it is not the most acidic or alkaline IL that induces the higher partition coefficient. Therefore, the effect of the pH of both phases in ABS on the partition coefficients can be considered negligible.

The increase of  $Na_2SO_4$  concentration reduces the solubility of L-tryptophan in the salt-rich phase (bottom phase), resulting in a further increase in the partitioning of amino acid to the top phase (PEG-rich phase).<sup>43-44</sup> The effect of  $Na_2SO_4$  concentration on the ABS extraction ability was studied for all the systems containing IL and for the control system without IL, and at 298.15 K. The results obtained are presented in Table 4. As a main example of the results obtained for the influence of the PEG 600 and

inorganic salt concentration, Fig. 9 presents the  $K_{Trp}$  values for the ABS with  $[im]Cl$  or  $[C_7H_7mim]Cl$ . Fig. 9 shows that the increase of the polymer concentration or salt concentration leads to an increase of  $K_{Trp}$ . As expected, the influence of the inorganic salt concentration leads to more pronounced differences in the  $K_{Trp}$  values than the influence of the PEG concentration.

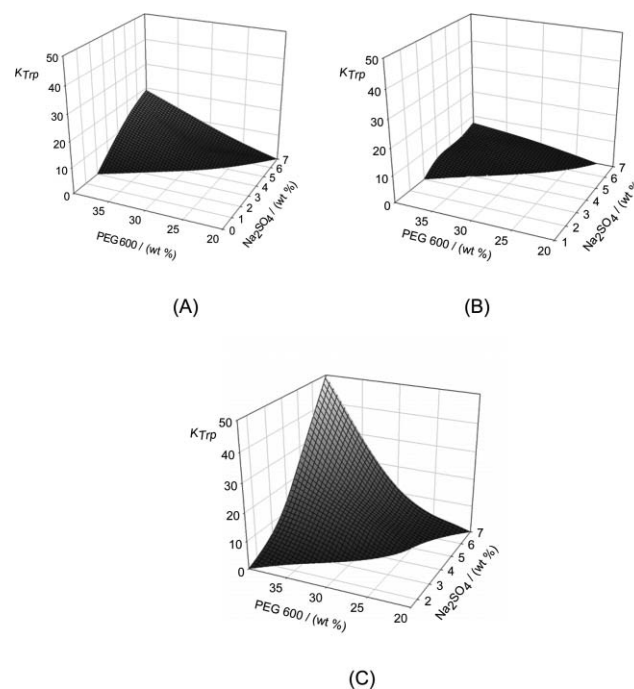


**Fig. 9** Partition coefficients of L-tryptophan as a function of PEG 600 and  $Na_2SO_4$  concentrations at 298.15 K: no IL (A); 5 wt% of  $[im]Cl$  (B); 5 wt%  $[C_7H_7mim][Cl]$  (C).

The concentration of IL added to the ABS system was also studied for the ILs  $[C_7H_7mim]Cl$  and  $[im]Cl$ , and at 298.15 K. These were chosen because they present the most extreme opposite behaviours of  $K_{Trp}$ . The results are reported in Table 7. When the  $[C_7H_7mim]Cl$  concentration is reduced from 5 to 2.5 wt% a decrease of only 20% on the partition coefficient of L-tryptophan is observed. This behaviour is followed by a negligible decrease of the  $K_{IL}$ . In contrast, when using  $[im]Cl$ , both partition coefficients decrease with the increase of the IL concentration but, while the  $K_{IL}$  falls by one half, the effect on  $K_{Trp}$  is still negligible.

**Table 7** Partition coefficients of L-tryptophan ( $K_{Trp}$ ) and IL ( $K_{IL}$ ) dependence on the IL concentration at 298.15 K

Quaternary System	Mass Fraction Composition/(wt%)			$K_{IL}$	$K_{Trp}$
	PEG 600	$Na_2SO_4$	IL		
$[im]Cl$	40.02	4.99	2.62	1.14	6.64
	39.96	5.00	5.08	0.48	5.54
	40.00	5.02	6.03	0.46	5.32
$[C_7H_7mim]Cl$	40.00	5.01	2.51	14.21	21.48
	39.94	5.03	5.00	15.01	25.92

## Conclusions

The use of ILs as adjuvants for the extraction of biomolecules using polymer-based ABS is proposed here. It is shown, using L-tryptophan as a model biomolecule, that ILs can be used to finely tune the phase behaviour and extraction capability of ABS through an appropriate choice of the IL employed. The effect of both the IL cation and anion on L-tryptophan extraction was established and the results can be extrapolated to other biomolecules of interest. The results reported suggest that the use of ILs as adjuvants to modify the characteristics of the polymer-rich phase could be an interesting alternative to the usual approach of PEG functionalization.

## Experimental section

### Materials

Na<sub>2</sub>SO<sub>4</sub> was purchased from LabSolve (purity > 99.8 wt%), and L-tryptophan (purity > 99.0 wt%) and polyethylene glycol 600 (PEG 600) were provided by Fluka. All reagents were of analytical grade. The following ionic liquids (ILs) were acquired at Iolitec: imidazolium chloride, [im]Cl; 1-methylimidazolium chloride, [C<sub>1</sub>mim]Cl; 1-ethyl-3-methylimidazolium chloride, [C<sub>2</sub>mim]Cl; 1-butyl-3-methylimidazolium chloride, [C<sub>4</sub>mim]Cl; 1-butyl-2,3-dimethylimidazolium chloride, [C<sub>4</sub>C<sub>1</sub>mim]Cl; 1-hydroxyethyl-3-methylimidazolium chloride, [OHC<sub>2</sub>mim]Cl; 1-allyl-3-methylimidazolium chloride, [amim]Cl; 1-benzyl-3-methylimidazolium chloride, [C<sub>7</sub>H<sub>7</sub>mim]Cl; 1-butyl-3-methylimidazolium acetate, [C<sub>4</sub>mim][CH<sub>3</sub>CO<sub>2</sub>]; 1-butyl-3-methylimidazolium methylsulfate, [C<sub>4</sub>mim][MeSO<sub>4</sub>]; 1-butyl-3-methylimidazolium hydrogenosulfate, [C<sub>4</sub>mim][HSO<sub>4</sub>]. Fig. 1 shows the chemical structure of the ILs studied. The ILs were dried under constant agitation under vacuum and at a moderate temperature (353 K), for a minimum of 48 h, to reduce the water and volatile compound content to negligible values. After this procedure, the purity of the ILs was further checked by <sup>1</sup>H and <sup>13</sup>C NMR spectra. A mass fraction purity above 99% was observed for all IL samples. The water used was double distilled, passed across a reverse osmosis system and further treated with a Milli-Q plus 185 water purification apparatus.

### Methods

**Phase diagrams and tie-lines.** Aqueous solutions of Na<sub>2</sub>SO<sub>4</sub> at 20 wt% + 5 wt% of each IL, aqueous solutions of PEG 600 at 40 wt% + 5 wt% of the same IL, and aqueous solutions of 5 wt% of IL were prepared and used for the determination of the binodal curves. The phase diagrams were determined through the cloud point titration method at 298 (± 1) K and atmospheric pressure. The experimental procedure adopted was previously used by us and is described in detail elsewhere.<sup>25-26</sup> The systems' composition was determined by the weight quantification of all components added within an uncertainty of ±10<sup>-5</sup> g.

The tie-lines were determined by a gravimetric method described by Merchuck *et al.*<sup>35</sup> For the TLs' determination a mixture at the biphasic region was prepared, vigorously stirred and allowed to reach equilibrium, by the separation of both phases, for 12 h at 298 K using small ampoules (*ca.* 10 cm<sup>3</sup>) especially designed for the purpose.<sup>25-26</sup> After the equilibration

step, the top and bottom phases were separated, recovered and weighed. Each individual TL was determined by application of the lever rule to the relationship between the top mass phase composition and the overall system composition. For that purpose the experimental binodal curves were correlated using eqn (1).<sup>35</sup>

The determination of the TLs was accomplished by solving the following system of four equations (eqns (7) to (10)) for the unknown values of Y<sub>T</sub>, Y<sub>B</sub>, X<sub>T</sub> and X<sub>B</sub>.

$$Y_T = A \exp[(BX_T^{0.5}) - (CX_T^3)] \quad (7)$$

$$Y_B = A \exp[(BX_B^{0.5}) - (CX_B^3)] \quad (8)$$

$$X_T = \frac{Y_M}{\alpha'} - \left(\frac{1-\alpha'}{\alpha'}\right)Y_B \quad (9)$$

$$X_B = \frac{X_M}{\alpha'} - \left(\frac{1-\alpha'}{\alpha'}\right)X_B \quad (10)$$

where *Y* and *X* are respectively, the PEG and inorganic salt weight percentages, and the subscript letters *T*, *B* and *M* represent the top, the bottom and the mixture phase, respectively. The parameter  $\alpha'$  is the ratio between the top and the total mass of the mixture.

The tie-line length (TLL) was determined according to eqn (11):

$$TLL = \sqrt{(X_T - X_B)^2 + (Y_T - Y_B)^2} \quad (11)$$

**Partitioning of L-tryptophan and ILs.** A mixture point in the biphasic region was selected and used to evaluate the L-tryptophan partitioning. An aqueous solution of L-tryptophan at 2.34 g·dm<sup>-3</sup> was used in the water content composition. After 5 min of gentle stirring, the biphasic system was allowed to equilibrate for 12 h immersed in a refrigerated water bath, Julabo F34, at each temperature of interest (278.15 K, 288.15 K, 298.15 K, 308.15 K and 318.15 K) within an uncertainty of ±0.01 K. After that period of equilibration the phases were clear and the interface well defined. The phases were thus carefully separated for further quantification of the amino acid and IL.

**Amino acid and IL quantification.** The L-tryptophan and IL concentrations, in the top and bottom phases, were determined using an UV spectrophotometer (SHIMADZU UV-1700), at a wavelength of 279 nm and 211 nm, respectively. Calibration curves were established for each compound. Possible interferences of the PEG 600, IL and Na<sub>2</sub>SO<sub>4</sub> in the L-tryptophan analytical method were taken into account and found to be of no significance at the dilutions carried out. Particularly for the aromatic ILs, the maximum peak of absorbance for the studied imidazolium-based ILs is at *ca.* 211 nm and, given the dilutions carried out in all phases, there was no contribution from the ILs to the absorbance at 279 nm.

**pH measurements.** After the partition of L-tryptophan and phase separation, the pH of each phase was determined using a pH Meter (Hanna Instruments, Model 9321) at 298 K, within an uncertainty of ±0.01.

## Acknowledgements

The authors are grateful to Coordenação de Aperfeiçoamento de Pessoal de Nível Superior (CAPES 2185/09-1) for the post-doctoral scholarship of A. S. Lima and to Fundação para a Ciência e a Tecnologia, SFRH/BPD/41781/2007 and SFRH/BD/60228/2009, for the post-doctoral and PhD scholarships of M. G. Freire and J. F. B. Pereira.

## References

- N. J. Bridges, K. E. Gutowski and R. D. Rogers, *Green Chem.*, 2007, **9**, 177–183.
- B. Bolognese, B. Nerli and G. N. Pico, *J. Chromatogr., B: Anal. Technol. Biomed. Life Sci.*, 2005, **814**, 347–353.
- X. C. Chen, G. M. Xu, X. Li, Z. J. Li and H. J. Ying, *Process Biochem.*, 2008, **43**, 765–768.
- M. M. Bora, S. Borthakur, P. C. Rao and N. N. Dutta, *Sep. Purif. Technol.*, 2005, **45**, 153–156.
- S. H. Li, C. Y. He, F. Gao, D. B. Li, Z. Chen, H. W. Liu, K. Li and F. Liu, *Talanta*, 2007, **71**, 784–789.
- P. Å. Albertsson, *Partition of cell particles and macromolecules: separation and purification of biomolecules, cell organelles, membranes, and cells in aqueous polymer two-phase systems and their use in biochemical analysis and biotechnology*, Wiley, New York, 1986.
- B. Y. Zaslavsky, *Aqueous two-phase partitioning, physical chemistry and bioanalytical applications*, Academic Press, New York, 1995.
- M. Rito-Palomares, *J. Chromatogr., B: Anal. Technol. Biomed. Life Sci.*, 2004, **807**, 3–11.
- M. Rito-Palomares, A. Negrete, L. Miranda, C. Flores, E. Galindo and L. Serrano-Carreón, *Enzyme Microb. Technol.*, 2001, **28**, 625–631.
- L. H. M. da Silva and A. J. A. Meirelles, *Carbohydr. Polym.*, 2000, **42**, 273–278.
- A. S. Lima, R. M. Alegre and A. J. A. Meirelles, *Carbohydr. Polym.*, 2002, **50**, 63–68.
- J. G. L. F. Alves, L. D. A. Chumpitaz, L. H. M. da Silva, T. T. Franco and A. J. A. Meirelles, *J. Chromatogr., B: Biomed. Sci. Appl.*, 2000, **743**, 235–239.
- D. Q. Lin, Y. T. Wu, L. H. Mel, Z. Q. Zhu and S. J. Yao, *Chem. Eng. Sci.*, 2003, **58**, 2963–2972.
- S. Zalipsky, *Bioconjugate Chem.*, 1995, **6**, 150–165.
- J. Li and W. J. Kao, *Biomacromolecules*, 2003, **4**, 1055–1067.
- P. A. J. Rosa, A. M. Azevedo, I. F. Ferreira, J. de Vries, R. Korpóraal, H. J. Verhoef, T. J. Visser and M. R. Aires-Barros, *J. Chromatogr., A*, 2007, **1162**, 103–113.
- A. M. Azevedo, P. A. J. Rosa, I. F. Ferreira, A. M. M. O. Pisco, J. de Vries, R. Korpóraal, T. J. Visser and M. R. Aires-Barros, *Sep. Purif. Technol.*, 2009, **65**, 31–39.
- Y. Y. Jiang, H. S. Xia, J. Yu, C. Guo and H. Z. Liu, *Chem. Eng. J.*, 2009, **147**, 22–26.
- C. Wu, J. J. Peng, J. Y. Li, Y. Bai, Y. Q. Hu and G. Q. Lai, *Catal. Commun.*, 2008, **10**, 248–250.
- K. E. Gutowski, G. A. Broker, H. D. Willauer, J. G. Huddleston, R. P. Swatloski, J. D. Holbrey and R. D. Rogers, *J. Am. Chem. Soc.*, 2003, **125**, 6632–6633.
- J. S. Wilkes, *Green Chem.*, 2002, **4**, 73–80.
- M. E. Zakrzewska, E. Bogel-Lukasik and R. Bogel-Lukasik, *Energy Fuels*, 2010, **24**, 737–745.
- U. Domańska and R. Bogel-Lukasik, *J. Phys. Chem. B*, 2005, **109**, 12124–12132.
- Y. U. Paulechka, G. J. Kabo, A. V. Blokhin, O. A. Vydrov, J. W. Magee and M. Frenkel, *J. Chem. Eng. Data*, 2003, **48**, 457–462.
- C. M. S. S. Neves, S. P. M. Ventura, M. G. Freire, I. M. Marrucho and J. A. P. Coutinho, *J. Phys. Chem. B*, 2009, **113**, 5194–5199.
- S. P. M. Ventura, C. M. S. S. Neves, M. G. Freire, I. M. Marrucho, J. Oliveira and J. A. P. Coutinho, *J. Phys. Chem. B*, 2009, **113**, 9304–9310.
- C. L. S. Louros, A. F. M. Cláudio, C. M. S. S. Neves, M. G. Freire, I. M. Marrucho, J. Pauly and J. A. P. Coutinho, *Int. J. Mol. Sci.*, 2010, **11**, 1777–1791.
- S. Dreyer and U. Kragl, *Biotechnol. Bioeng.*, 2008, **99**, 1416–1424.
- S. Li, C. He, H. Liu, K. Li and F. Liu, *J. Chromatogr., B: Anal. Technol. Biomed. Life Sci.*, 2005, **826**, 58–62.
- C. He, S. Li, H. Liu, K. Li and F. Liu, *J. Chromatogr., A*, 2005, **1082**, 143–149.
- V. Najdanovic-Visak, A. Rodriguez, Z. P. Visak, J. N. Rosa, C. A. M. Afonso, M. N. da Ponte and L. P. N. Rebelo, *Fluid Phase Equilib.*, 2007, **254**, 35–41.
- A. Soto, A. Arce and M. K. Khoshkbarchi, *Sep. Purif. Technol.*, 2005, **44**, 242–246.
- M. G. Freire, C. M. S. S. Neves, P. J. Carvalho, R. L. Gardas, A. M. Fernandes, I. M. Marrucho, L. M. N. B. F. Santos and J. A. P. Coutinho, *J. Phys. Chem. B*, 2007, **111**, 13082–13089.
- J. G. Huddleston, A. E. Visser, W. M. Reichert, H. D. Willauer, G. A. Broker and R. D. Rogers, *Green Chem.*, 2001, **3**, 156–164.
- J. C. Merchuk, B. A. Andrews and J. A. Asenjo, *J. Chromatogr., B: Biomed. Sci. Appl.*, 1998, **711**, 285–293.
- M. G. Freire, C. M. S. S. Neves, A. M. S. Silva, L. M. N. B. F. Santos, I. M. Marrucho, L. P. N. Rebelo, J. K. Shah, E. J. Maginn and J. A. P. Coutinho, *J. Phys. Chem. B*, 2010, **114**, 2004–2014.
- N. Le Floch and B. Seve, *Livestock Science*, 2007, **112**, 23–32.
- Y. Nozaki and C. Tanford, *J. Biol. Chem.*, 1971, **246**, 2211–2217.
- M. A. Eiteman and J. L. Gainer, *Abstr. Pap. Am. Chem. S.*, 1990, **200**, 116.
- Y. C. Pei, J. J. Wang, K. Wu, X. P. Xuan and X. J. Lu, *Sep. Purif. Technol.*, 2009, **64**, 288–295.
- D. Sadava, H. C. Heller, D. M. Hillis, M. Berenbaum, *Life: The Science of Biology*, W. H. Freeman, New York, 2009.
- L. I. N. Tomé, V. R. Catambas, A. R. Teles, M. G. Freire, I. M. Marrucho and J. A. P. Coutinho, *Sep. Purif. Technol.*, 2010, **72**, 167–173.
- B. R. Babu, N. K. Rastogi and K. S. M. S. Raghavarao, *Chem. Eng. Process.*, 2008, **47**, 83–89.
- R. Kuboi, H. Tanaka and I. Komasa, *Kagaku Kagaku Ronbun.*, 1991, **17**, 67–74.